PHYSICAL REVIEW D **87,** 011105(R) (2013)

Laboratory search for spin-dependent short-range force from axionlike particles using optically polarized ^{3}He gas

P.-H. Chu,[1,*] A. Dennis,[2] C. B. Fu,[3] H. Gao,[1] R. Khatiwada,[2] G. Laskaris,[1] K. Li,[2] E. Smith,[2] W. M. Snow,[2] H. Yan,[2] and W. Zheng[1]

[1]*Triangle Universities Nuclear Laboratory and Department of Physics, Duke University, Durham, North Carolina 27708, USA*
[2]*Department of Physics, Indiana University, Bloomington, Indiana 47408, USA*
[3]*Department of Physics, Shanghai Jiaotong University, Shanghai 200240, China*

(Received 6 November 2012; published 31 January 2013)

The possible existence of short-range forces between unpolarized and polarized spin-$\frac{1}{2}$ particles has attracted the attention of physicists for decades. These forces are predicted in various theories and provide a possible new source for parity and time-reversal symmetry violation. We use an ensemble of polarized ^{3}He gas in a cell with a 250-μm thick glass window to search for a force from pseudoscalar boson exchange over sub-millimeter ranges. This interaction would produce an NMR frequency shift as an unpolarized mass is moved near and far from the polarized ensemble. We report a new upper bound with a factor of 10–30 improvement on the product $g_s g_p^n$ of the scalar couplings to the fermions in the unpolarized mass, and the pseudoscalar coupling of the polarized neutron in the ^{3}He nucleus for force ranges from 10^{-4} to 10^{-2} m, which corresponds to a mass range of 2×10^{-3} to 2×10^{-5} eV for the pseudoscalar boson. This represents the most sensitive search that sets a direct limit on the important "axion window."

DOI: 10.1103/PhysRevD.87.011105 PACS numbers: 14.80.Va, 13.75.Cs, 24.80.+y

Possible short-range forces between unpolarized and polarized spin-$\frac{1}{2}$ particles can provide a new source for parity (P) and time-reversal (T) symmetry violation [1]. Moody and Wilczek [2] proposed a force from the exchange of spin-0 bosons which can couple to fermions through scalar and pseudoscalar vertices. The scalar coupling is spin-independent and depends only on the fermion density. The pseudoscalar coupling is entirely spin-dependent. The resulting spin-dependent short-range force (SDSRF) has a Yukawa-type interaction potential from one boson exchange of the form

$$V(r) = \frac{g_s g_p \hbar^2}{8\pi m_p}(\hat{\sigma}\cdot\hat{r})\left(\frac{1}{r\lambda}+\frac{1}{r^2}\right)\exp(-r/\lambda), \qquad (1)$$

where $\hat{r}$ is the unit vector from the unpolarized particle to the polarized particle, $\hat{\sigma}$ is the spin of the polarized particle, m_p is the polarized particle mass, $g_s g_p$ is the product of couplings of the scalar vertex in the unpolarized matter and the pseudoscalar vertex of the polarized particle, and λ is the force range. Such forces may be induced by pseudoscalar bosons like the axion [3], axion-like-particles (ALPs) [4], or a very light spin-1 boson [5] which are candidates for cold dark matter [6]. Current experimental and astrophysical observation restricts the axion mass to between 1 μeV and 1 meV, corresponding to a force range between 2 cm and 20 μm, the so-called axion window [7]. Many ALPs, predicted by string theory [8] and many extensions to the standard model [9,10], also predict weak forces in this range.

Several experiments have been performed to search for SDSRFs using different techniques. Some examples include the torsion pendulum [11–13], neutron bound states on a mirror in the Earth's gravitational field [14], and longitudinal and transverse spin relaxation of polarized neutrons and ^{3}He [15–18]. A potential of the form $\hat{\sigma}\cdot\hat{r}$ can introduce a shift in the precession frequency of polarized particles in the presence of an unpolarized mass [19,20], similar to that of a magnetic dipole in an external magnetic field, $\propto \vec{\mu}\cdot\vec{B}$. The first measurement using this idea with ^{3}He [21] achieved a sensitivity of 5×10^{-3} Hz and restricted the coupling strength close to the current limit for force ranges from 10^{-4} to 10^{-2} m without any magnetic shielding. In this work, we present new results with a factor of 10–30 increase in sensitivity which constitute, to our knowledge, the most stringent laboratory limit on $g_s g_p^n$ in the important axion window. The spin of the ^{3}He is dominated by the spin of the neutron [22] so this result is directly interpretable in terms of the coupling g_p^n. Constraints on T-odd and P-odd interactions of the ^{3}He atom from bounds on the electric dipole moment (EDM) of its constituents from new physics at high-energy scales are highly suppressed due to the Schiff's screening [23] and the cancellation of the electronic EDM in the ground state of the ^{3}He atom. Our work therefore also represents to our knowledge the most sensitive search for T-odd and P-odd interactions in the ^{3}He atom at low energies.

The apparatus used in this work is based on the design of Ref. [21]. We use a 7 amg high-pressure ^{3}He cell as shown in Fig. 1, which has an optical pumping chamber and a target chamber connected by a glass tube. ^{3}He is polarized using spin-exchange optical pumping [24] in the spherical

*pc102@duke.edu

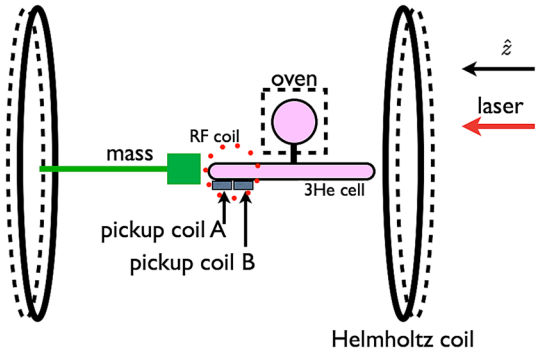

FIG. 1 (color online). Schematic of the SDSRF experiment (not to scale). The cylindrical polarized ^{3}He cell is located in a uniform magnetic field. Correction coils (dashed-loop curves) compensate for residual holding-field gradients. The direction of the laser and the holding field are along $\hat{z}$.

pumping chamber of radius 4.3 cm. The polarized ^{3}He atoms diffuse into the lower 40-cm long cylindrical chamber, which possesses two hemispherical glass windows at both ends with a thickness of 250 μm.

We describe below a number of experimental improvements compared to Ref. [21], which enhance the sensitivity to SDSRFs. A pair of correction coils is applied to the Helmholtz coils to improve the uniformity of the holding field. Two identical pickup coils A and B of 2.5-cm diameter are located next to each other at the same end of the ^{3}He cell. Pickup coil A is mounted below the window to measure the precession frequency shift of the polarized ^{3}He nuclei due to an SDSRF from the unpolarized mass. Pickup coil B is positioned to be insensitive to an SDSRF; its signal is used to monitor the holding-field drift. We subtract the frequencies measured in both coils and form $f'_A = f_A - f_B$ for each measurement. The ^{3}He cell position relative to the Helmholtz coils is adjusted to optimize the transverse spin relaxation time T_2 measured from coil A and B.

The holding field is tuned to produce a ^{3}He Larmor frequency near 23.8 kHz. We apply a 24-kHz rf pulse to tip the spins by a small angle with negligible polarization loss. The polarized ^{3}He nuclei induce emf's in the pickup coils which are digitized and recorded. The precession frequency is determined first by applying a Fourier transform to a signal $s(t)$ in the time domain and obtaining the real and the imaginary parts of the signal in the frequency domain as $R(f)$ and $I(f)$, respectively. The Fourier transform is numerically calculated using Richardson extrapolation [25]. The total amplitude is $S(f) = \sqrt{R^2(f) + I^2(f)}$. The reference frequency f is then varied with a 10^{-6} Hz step to locate the maximum of $S(f)$, which is the precession frequency [26].

Two samples are used as the unpolarized masses: a Macor ceramic mass block of dimensions $34 \times 52 \times 38$ mm^3 used in Ref. [21] and a liquid mixture of 1.02% $MnCl_2$ in pure water. These samples are chosen for their different nucleon densities, low magnetic impurities and magnetic susceptibilities, and minimal influence on the nuclear magnetic resonance (NMR) measurement procedure. The paramagnetic salt is added in order to compensate for the diamagnetism of the water. The magnetic susceptibility of this mixture is measured to be $<5\%$ of that of pure water. A stepping motor is used to move the ceramic mass a distance of 5 cm to 10 μm from the target chamber window. The salt water is stored in a cylindrical polytetrafluoroethylene (PTFE) tank of radius 34 mm and length 37 mm. Its one end is sealed with a 25-μm flexible PTFE film, which contacts the target chamber window. The other end of the liquid tank is connected to a flexible PTFE tube, which moves the liquid in and out of the tank using a nonmagnetic air cylinder actuated by a magnetically shielded switch.

In this work, we also improved the analysis method, which is described below. We define a mass-in state (in) or mass-out state (out) with the mass close to or away from the chamber window. Each measurement cycle employs two states of the mass position in the sequence (in, out, in, out) with a 60-second pause in the middle. We apply the analysis algorithm presented in Ref. [27] to derive the frequency difference between the two states and remove any possible bias from linear or quadratic time-dependent frequency drifts. Assuming linear and quadratic time-dependent frequency drifts $f(t) \propto at + bt^2 \pm c$, with a and b being arbitrary constants and $+c(-c)$ the frequency shift depending on the in(out) state, the frequency difference between two successive cycles 1 and 2 is given by

$$\begin{aligned}\Delta f &= \frac{1}{4}[f_{\mathrm{in},1} - 3f_{\mathrm{out},1} + 3f_{\mathrm{in},2} - f_{\mathrm{out},2}] \\ &= \frac{1}{4}[(a\delta t + b\delta t^2 + c) - 3(a(2\delta t) + b(2\delta t)^2 - c) \\ &\quad + 3(a(3\delta t) + b(3\delta t)^2 + c) - (a(4\delta t) + b(4\delta t)^2 - c)] \\ &= 2c, \end{aligned} \tag{2}$$

where δt is the measurement time step (the time at the beginning of the first step of cycle 1 is taken as zero) and $f_{\mathrm{in/out},1/2}$ is the frequency measured in the pickup coil A minus the pickup coil B for cycles 1 and 2, respectively. Higher-order algorithms produced the same results.

The mass in-mass out frequency difference can be measured in four different configurations of the apparatus corresponding to the directions of the main holding field and of the ^{3}He polarization [21], each of which should possess the same magnitude of a frequency shift in the presence of a nonzero SDSRF proportional to the nucleon density of the mass. However, for our apparatus, two of these configurations possess residual field gradients in the sample large enough to lower the spin relaxation time T_2 and produce complicated line shapes whose frequency shifts—determined by a peak-finding algorithm of the type used in our analysis—are too sensitive to possible

magnetic systematic effects induced by the mass. We therefore consider only two of the four configurations of the apparatus which lead to a longer spin relaxation time T_2.

We define the precession frequency in different configurations of the holding field and the polarization direction as $f_{B,P}$, where the holding field $B = \pm$ and the polarization direction $P = \pm$. The precession induced by the SDSRF does not change after reversing the holding field, assuming the holding-field rotation does not change the polarization of the ^{3}He. But its precession direction now becomes opposite to the magnetic field-induced precession. Any systematic effects depending only on the polarization direction do not change after reversing the holding field. For different configurations, we can write

$$\begin{aligned} f_{+\pm} &= f_B \pm \Delta f_P + \Delta f_{\mathrm{SDSRF}}, \\ f_{-\mp} &= f_B \pm \Delta f_P - \Delta f_{\mathrm{SDSRF}}, \end{aligned} \tag{3}$$

where f_B is the magnetic field-dependent precession frequency including the holding field and the possible effect from the magnetic susceptibility of the mass, Δf_P is the polarization-dependent frequency shift, and $\Delta f_{\mathrm{SDSRF}}$ represents the frequency shift due to the SDSRF. In this work, the two configurations $(+\ -)$ and $(-\ +)$, which both have clean line shapes, are considered in determining the SDSRF:

$$\Delta f_{\mathrm{SDSRF}} = \frac{1}{2}(\Delta f_{+-} - \Delta f_{-+}), \tag{4}$$

where Δf_{+-} and Δf_{-+} are the frequency differences between the mass-in and mass-out states and the frequency measured in the pickup coil A minus the pickup coil B of each configuration.

We take 1000 cycles continuously for each configuration of each sample. The uncertainty in the measured frequency shift is given by $\frac{1}{2}\sqrt{\sigma_{+-}^2 + \sigma_{-+}^2}$. Figure 2 and Table I show the data of two samples and the average frequency shift due to the SDSRF. The result shows that the average frequency difference of the salt water is consistent with zero.

Based on these results, we can constrain the force range and the coupling strength. The precession frequency shift due to the SDSRF for each polarized ^{3}He nucleus in the target chamber can be calculated by numerically integrating Eq. (1) over the unpolarized mass as

$$\Delta f(\vec{z}, \lambda, g_s g_p^n) = \frac{2N}{2\pi\hbar} \int_{\mathrm{vol}} V(\vec{r} - \vec{z}) dr^3, \tag{5}$$

where N is the particle number density of the unpolarized mass, vol is the total volume of the unpolarized mass, and $\vec{z}$ is the distance from the surface of the mass to the polarized ^{3}He nucleus. The precession signal measured by the pickup coil is $s(t) \propto \int (\vec{B}_{\mathrm{coil}} \cdot \partial \vec{M}/\partial t) dr^3$, where $\vec{M}$ is the magnetization vector of ^{3}He and $\vec{B}_{\mathrm{coil}}$ is the field profile of the pickup coil, which can be derived by using the reciprocity theorem [28]. The signal is written as

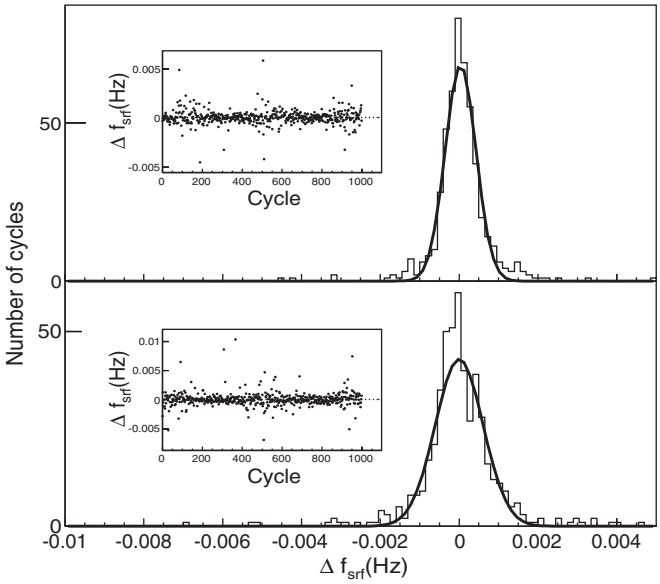

FIG. 2. Frequency difference of Macor ceramic (top) and salt water (bottom) for 1000 cycles. The average Δf_{srf} is obtained by fitting the distribution as a Gaussian function. Small boxes show the Δf_{srf} verse cycle.

$$\begin{aligned} s(t) = C\Big\{\int_d & -B_x \cdot (f_0 + \Delta f)\sin(2\pi(f_0 + \Delta f)t) \\ & + B_y \cdot (f_0 + \Delta f)\cos(2\pi(f_0 + \Delta f)t) dz\Big\}, \end{aligned} \tag{6}$$

where $f_0 = \gamma B_0/2\pi$ is the Larmor frequency, $\gamma/2\pi = -3.24$ Hz/mG is the gyromagnetic ratio of ^{3}He, d is the thickness of the cell window, and C is a constant. Applying the Fourier transformation, the power spectrum of the signal can be calculated as

$$\begin{aligned} P(f') = C\Big\{\Big(\int (f_0 + \Delta f) B_x \delta(f_0 + \Delta f - f') dz\Big)^2 \\ + \Big(\int (f_0 + \Delta f) B_y \delta(f_0 + \Delta f - f') dz\Big)^2\Big\}. \end{aligned} \tag{7}$$

The average frequency observed by the pickup coil is

$$\bar{f}' = \frac{\int f' P(f') df'}{\int P(f') df'}. \tag{8}$$

TABLE I. Data of each configuration of two samples. $\Delta f_{B,P}$ is the average frequency difference between mass-in and -out states and the frequency measured in the pickup coil A minus the pickup coil B of each configuration.

	$\Delta f_{B,P}$		
Sample	$+\ -\ [10^{-5}$ Hz]	$-\ +\ [10^{-5}$ Hz]	$\Delta f_{\mathrm{srf}}[10^{-5}$ Hz]
Ceramic	0.6 ± 1.3	-4.6 ± 3.1	2.6 ± 1.7
Salt water	-3.3 ± 0.8	-1.7 ± 5.2	-0.8 ± 2.6

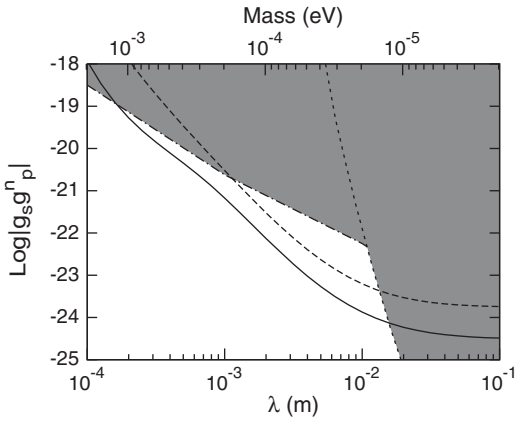

FIG. 3. Constraints on the coupling strength $g_s g_p^n$ as a function of the force range λ and the equivalent mass of the ALPs. The dark gray area is the region excluded by previous works. The dotted curve is from Ref. [19] and the dash-dotted curve is from Ref. [17]. The dashed (solid) curve is the constraint of the salt water (ceramic) sample within one standard deviation.

The frequency shift due to the SDSRF is $\Delta\bar{f}(\lambda, g_s g_p^n) = \bar{f}' - f_0$. Using the measured frequency difference in Table I, the constraint on the coupling strength and the force range is determined as shown in Fig. 3 where the dark gray area was ruled out by previous measurements. The dotted curve is from Ref. [19] and the dash-dotted curve is from Ref. [17]. The dashed (solid) curve is the constraint of the salt water (ceramic) sample within one standard deviation. The measured frequency difference of the ceramic sample due to the SDSRF is consistent with zero within 1.5 standard deviations. Our new results improve the constraint on the SDSRF from the current limit in the range of 10^{-4} to 10^{-2} m by a factor of 10–30, which corresponds to a mass range of 2×10^{-3} to 2×10^{-5} eV for the pseudoscalar boson involved. This work represents the most sensitive search that sets a direct limit on the important axion window.

Several methods can be employed in the future to further improve the sensitivity using polarized ^{3}He. Obvious paths for improvement of the measurement include new magnetic holding-field systems with better field uniformity and magnetic shielding, a smaller ^{3}He cell with a lower pressure and thinner windows, unpolarized mass samples with higher fermion densities and lower magnetic susceptibilities, and a $X^{129}e$ comagnetometer. With these changes, we conclude that a factor of 10–100 improvement in the constraints of the coupling strength in the force range of 10^{-4} to 10^{-2} m is possible.

The authors thank M. Souza and T. Averett for their help with the construction of the ^{3}He cell. The authors also thank Y. Zhang, S. Jawalkar, T. Gentile, M. Yu. Khlopov, and P. Fayet for helpful discussions. This work was supported by the Duke University, the U.S. Department of Energy under Contract DE-FG02-03ER41231, and the U.S. National Science Foundation through Grant No. PHY-1068712. K. Li, R. Khatiwada, E. Smith, M. Snow, and H. Yan acknowledge support from the Indiana University Center for Spacetime Symmetries and A. Dennis from the IU STARS program.

[1] J. Leitner and S. Okubo, Phys. Rev. B **136**, B1542 (1964).
[2] J. E. Moody and F. Wilczek, Phys. Rev. D **30**, 130 (1984).
[3] R. D. Peccei and H. R. Quinn, Phys. Rev. Lett. **38**, 1440 (1977).
[4] J. Jaeckel and A. Ringwald, Annu. Rev. Nucl. Part. Sci. **60**, 405 (2010).
[5] P. Fayet, Classical Quantum Gravity **13**, A19 (1996).
[6] E. W. Kolb and M. S. Turner, *The Early Universe* (Addison-Wesley, Redwood, CA, 1990).
[7] I. Antoniadis, S. Baessler, M. Büchner, V. V. Fedorov, S. Hoedl, A. Lambrecht, V. V. Nesvizhevsky, G. Pignol, K. V. Protasov, S. Reynaud, and Y. Sobolev, C.R. Physique **12**, 755 (2011).
[8] P. Svrcek and E. Witten, J. High Energy Phys. 06 (2006) 051.
[9] B. A. Dobrescu and I. Mocioiu, J. High Energy Phys. 11 (2006) 005.
[10] E. G. Adelberger, J. H. Gundlach, B. R. Heckel, S. Hoedl, and S. Schlamminger, Prog. Part. Nucl. Phys. **62**, 102 (2009).
[11] R. C. Ritter, L. I. Winkler, and G. T. Gillies, Phys. Rev. Lett. **70**, 701 (1993).
[12] G. D. Hammond, C. C. Speake, C. Trenkel, and A. P. Patón, Phys. Rev. Lett. **98**, 081101 (2007).
[13] S. A. Hoedl, F. Fleischer, E. G. Adelberger, and B. R. Heckel, Phys. Rev. Lett. **106**, 041801 (2011).
[14] S. Baeßler, V. V. Nesvizhevsky, K. V. Protasov, and A. Yu. Voronin, Phys. Rev. D **75**, 075006 (2007).
[15] A. P. Serebrov, Phys. Lett. B **680**, 423 (2009)
[16] Y. N. Pokotilovski, Phys. Lett. B **686**, 114 (2010).
[17] A. Petukhov, G. Pignol, D. Jullien, and K. Andersen, Phys. Rev. Lett. **105**, 3 (2010).
[18] C. B. Fu, T. R. Gentile, and W. M. Snow, Phys. Rev. D **83**, 031504(R) (2011); A. K. Petukhov, G. Pignol, and R. Golub, Phys. Rev. D **84**, 058501 (2011).
[19] A. N. Youdin, D. Krause, Jr., K. Jagannathan, L. R. Hunter, and S. K. Lamoreaux, Phys. Rev. Lett. **77**, 2170 (1996).
[20] W.-T. Ni, S.-S. Pan, H.-C. Yeh, L.-S. Hou, and J. Wan, Phys. Rev. Lett. **82**, 2439 (1999).
[21] W. Zheng, H. Gao, B. Lalremruata, Y. Zhang, G. Laskaris, W. M. Snow, and C. Fu, Phys. Rev. D **85**, 031505 (2012).
[22] J. L. Friar, B. F. Gibson, G. L. Payne, A. M. Bernstein, and T. E. Chupp, Phys. Rev. C **42**, 2310 (1990).
[23] L. Schiff, Phys. Rev. **132**, 2194 (1963).

[24] T. G. Walker and W. Happer, Rev. Mod. Phys. **69**, 629 (1997).

[25] L. F. Richardson, Phil. Trans. R. Soc. A **210**, 307 (1911); L. F. Richardson and J. A. Gaunt, Phil. Trans. R. Soc. A **226**, 299 (1927).

[26] H. Yan *et al.* (unpublished).

[27] H. E. Swanson and S. Schlamminger, Meas. Sci. Technol. **21**, 115104 (2010).

[28] E. K. Insko, M. A. Elliott, J. C. Schotland, and J. S. Leigh, J. Magn. Reson. **131**, 111 (1998).